

IRON EMISSION IN THE $Z = 6.4$ QUASAR SDSS J114816.64+525150.3AARON J. BARTH^{1,2}, PAUL MARTINI³, CHARLES H. NELSON⁴, AND LUIS C. HO³

ABSTRACT

We present near-infrared J and K -band spectra of the $z = 6.4$ quasar SDSS J114816.64+525150.3 obtained with the NIRSPEC spectrograph at the Keck-II telescope, covering the rest-frame spectral regions surrounding the C IV $\lambda 1549$ and Mg II $\lambda 2800$ emission lines. The iron emission blend at rest wavelength 2900–3000 Å is clearly detected and its strength appears nearly indistinguishable from that of typical quasars at lower redshifts. The Fe II/Mg II ratio is also similar to values found for lower-redshift quasars, demonstrating that there is no strong evolution in Fe/ α broad-line emission ratios even out to $z = 6.4$. In the context of current models for iron enrichment from Type Ia supernovae, this implies that the SN Ia progenitor stars formed at $z \gtrsim 10$. We apply the scaling relations of Vestergaard and of McLure & Jarvis to estimate the black hole mass from the widths of the C IV and Mg II emission lines and the ultraviolet continuum luminosity. The derived mass is in the range $(2-6) \times 10^9 M_{\odot}$, with an additional uncertainty of a factor of 3 due to the intrinsic scatter in the scaling relations. This result is in agreement with the previous mass estimate of $3 \times 10^9 M_{\odot}$ by Willott, McLure, & Jarvis, and supports their conclusion that the quasar is radiating close to its Eddington luminosity.

Subject headings: quasars: emission lines — quasars: individual (SDSS J114816.64+525150.3)

1. INTRODUCTION

The broad emission lines of high-redshift quasars are luminous beacons that can be used to study the metal enrichment history of the densest regions in the early universe (e.g., Hamann & Ferland 1999). Observations of emission lines such as C IV and N V reveal supersolar abundances in quasar broad-line regions (BLRs) even at $z > 4$ (Dietrich et al. 2003a), strengthening the link between the growth and fueling of black holes and the buildup of stellar mass in the host galaxies. The abundance ratio of iron to α elements is a key diagnostic that may be used as a “clock” to constrain the earliest epoch of star formation (Hamann & Ferland 1993; Yoshii et al. 1998), since enrichment of α elements occurs via core-collapse supernovae while the dominant channel for iron enrichment is Type Ia supernovae, which have longer-lived progenitor stars.

The flux ratio of the integrated iron emission in the 2200–3000 Å wavelength range to Mg II $\lambda\lambda 2796, 2802$ is an observationally accessible diagnostic that is dependent on the underlying Fe/Mg abundance ratio, but also sensitive to the BLR density and microturbulence (Verner et al. 2003). Numerous studies have demonstrated that there is no systematic decrease in the Fe II/Mg II flux ratio of quasars with increasing redshift, even out to $z \approx 6$ (e.g., Thompson, Hill, & Elston 1999; Dietrich et al. 2002, 2003b; Freudling et al. 2003), while Iwamuro et al. (2002) found evidence for an *increase* in Fe II/Mg II with increasing redshift to $z \approx 5$.

SDSS J114816.64+525150.3 (abbreviated here as SDSS J1148+5251) was discovered by Fan et al. (2003) in the Sloan Digital Sky Survey; at $z = 6.4$ it is the highest-redshift quasar currently known. Willott et al. (2003) used H and K -band spectra of this object to obtain an estimate of the black hole mass ($\sim 3 \times 10^9 M_{\odot}$) from the Mg II linewidth, using the scaling relations derived by McLure & Jarvis (2002). The Mg II $\lambda 2800$ line was the only emission feature clearly present in their spectrum;

the limited S/N of their data did not permit a definitive detection of the surrounding Fe II emission blends. The quasar environment was evidently a site of vigorous massive star formation and metal enrichment prior to $z = 6.4$, as demonstrated by the roughly normal equivalent width of the Mg II emission line as well as the presence of submillimeter emission from $10^8 M_{\odot}$ of dust in the quasar host galaxy (Bertoldi et al. 2003). Here, we present new near-infrared spectra of SDSS J1148+5251 obtained at the Keck Observatory, covering the rest-frame spectral regions surrounding the C IV $\lambda 1549$ and Mg II $\lambda 2800$ emission lines. We show that its Fe II/Mg II ratio is similar to that of typical quasars at lower redshifts, and we update the black hole mass estimate of Willott et al. using the higher-quality Keck data. Except where noted otherwise, we assume $H_0 = 70 \text{ km s}^{-1} \text{ Mpc}^{-1}$, $\Omega_m = 0.3$, and $\Omega_{\Lambda} = 0.7$; for this cosmology the universe at $z = 6.4$ was 840 Myr old.

2. OBSERVATIONS AND REDUCTIONS

The observations were obtained using the NIRSPEC spectrograph (McLean et al. 2000) at the Keck-II telescope on the nights of 2003 March 11 and 12 UT. We used a $0''.76$ -wide slit in the NIRSPEC-1, 2, and 6 settings, which cover the wavelength ranges 0.95–1.12, 1.08–1.29, and 1.89–2.31 μm , respectively, at $R \approx 1500$. A standard ABBA nodding sequence was used with exposure times of 300 s at each nod position. The airmass ranged from 1.2 to 1.5. Seeing, as measured from the spatial profiles of calibration star exposures, was typically between $0''.7$ and $0''.9$. The total exposure times in each setting were 6000, 9600, and 8400 s, respectively. Due to hardware problems, the nodding and guiding performance of NIRSPEC was relatively poor during this run and slit losses were severe, possibly $\sim 50\%$ during some individual exposures.

The spectra were extracted from bias-subtracted, flattened 2-dimensional frames using an optimal weighting algorithm, and using the sky-subtraction code of Kelson (2003). Wavelength

¹ Caltech Optical Observatories, 105-24 Caltech, Pasadena, CA 91125

² Hubble Fellow

³ The Observatories of the Carnegie Institution of Washington, 813 Santa Barbara Street, Pasadena, CA 91101

⁴ Department of Physics and Astronomy, Drake University, 2507 University Avenue, Des Moines, IA 50311-4505

calibration was performed with the OH airglow emission lines in each exposure. The data were flux-calibrated and corrected for telluric absorption using spectra of the A0V star HD 99966, observed immediately before or after the quasar in each setting, following the methods described by Vacca, Cushing, & Rayner (2003). Finally, the spectra were scaled to the J and K' magnitudes given for SDSS J1148+5251 by Fan et al. (2003), to place them on an absolute flux scale.

3. RESULTS AND DISCUSSION

The spectra are displayed in Figure 1, overplotted with the SDSS composite quasar spectrum of Vanden Berk et al. (2001). The best match between the Mg II profile of SDSS J1148+5251 and the SDSS composite is found for a redshift of 6.40 ± 0.01 , in agreement with the previous measurement of $z = 6.41 \pm 0.01$ by Willott et al. (2003). However, the C IV emission line appears strongly blueshifted with respect to the Mg II redshift and is much broader than the C IV line of the composite quasar. The C IV line falls within a telluric absorption band at $1.14 \mu\text{m}$, making accurate flux calibration difficult, but the extended blue wing of C IV does appear to be a real feature in the spectrum. In quasars, Mg II is considered a good indicator of the systemic redshift while relative C IV blueshifts of $500\text{--}2000 \text{ km s}^{-1}$ or more are common (Marziani et al. 1996; Richards et al. 2002). The centroid of the C IV line measured by a Gaussian fit corresponds to a blueshift of $2900 \pm 120 \text{ km s}^{-1}$ relative to the Mg II line. Richards et al. (2002) find that the Si IV $\lambda 1400$ emission line of quasars is typically not strongly blueshifted, unlike C IV; Figure 1 shows that SDSS J1148+5251 appears to follow this trend.

The data do not reveal any broad absorption lines, but a few narrow absorption lines are present. The strongest are at $1.0853 \mu\text{m}$ (equivalent width $5.6 \pm 0.8 \text{ \AA}$) and at $1.1842 \mu\text{m}$ (equivalent width $4.4 \pm 0.4 \text{ \AA}$). Neither is coincident with an atmospheric absorption or emission feature, and they appear to be genuine features in the quasar spectrum. The line at $1.1842 \mu\text{m}$ is unresolved, while the $1.0853 \mu\text{m}$ feature is marginally broader than the night sky emission lines but not broad enough to be consistent with a blended C IV or Mg II doublet. The identification of these lines is uncertain, and neither of them matches any wavelengths that would be expected for metal absorption lines from the $z = 4.943$ C IV absorber found by White et al. (2003).

3.1. Fe II Emission

In general, measurement of the iron emission strength is best accomplished when the data have wide spectral coverage, so that spectral regions without either iron emission or Balmer continuum emission can be included in the fit (e.g., Dietrich et al. 2002). Our spectrum does not extend to sufficiently long wavelengths to do this, and we fit only the rest-frame spectral region $2610\text{--}3100 \text{ \AA}$. An Fe II emission blend at $2900\text{--}3000 \text{ \AA}$ is clearly present in the Keck spectrum. From the comparison between the NIRSPEC data and the SDSS composite spectrum in Figure 1, it is already apparent that the Fe II/Mg II ratio in SDSS 1148+5251 is roughly similar to that in the composite quasar.

The spectrum was modeled as the sum of three components: a power-law continuum, an empirical iron emission template, and a double-Gaussian model for the Mg II profile. For the Mg II model, all of the Gaussian parameters were allowed to

float freely. We do not ascribe any particular physical interpretation to the two components in terms of the structure of the emission-line regions; this is simply the minimal empirical description that allows an adequate fit to the emission line. Dietrich et al. (2002) show that the Mg II profiles of quasars can generally be fit well by a Gaussian near the systemic velocity plus another blueshifted (and usually broader) Gaussian component. We note that the model fit may be affected by an imperfect correction for telluric absorption in the blue wing of Mg II. Given our limited spectral coverage we chose not to include the Balmer continuum emission as a separate component, since its strength could not be determined independently of the dominant power-law continuum.

The iron blends in this wavelength region are traditionally modeled using an empirical “template” spectrum derived from an AGN with intrinsically narrow emission lines. We used an iron template derived from *HST* ultraviolet observations of I Zw 1 as described by Vestergaard & Wilkes (2001)⁵; the iron emission is dominated by Fe II blends with a contribution from Fe III. The iron template was broadened by convolution with a Gaussian having the same width as the stronger Mg II component. To optimize the fit we computed a χ^2 parameter determined using the 1σ uncertainties on each pixel in the flux-calibrated spectra. Figure 2 displays the best-fitting model. The power-law index of the model continuum is $\alpha = -1.4 \pm 0.1$ for $f_\lambda \propto \lambda^\alpha$, similar to the value of $\alpha = -1.56$ for the SDSS composite quasar (Vanden Berk et al. 2001).

Following Dietrich et al. (2002), the Fe II/Mg II emission-line ratio was determined by integrating the iron template flux over the wavelength range $2200\text{--}3090 \text{ \AA}$. Although this requires extrapolation of the scaled iron template beyond the wavelength range over which our fit was performed, it allows the most straightforward comparison with previous measurements. We find $\text{Fe II/Mg II} = 4.7 \pm 0.4$. This result is similar to values that have been found for quasars over all observed redshifts. For example, Dietrich et al. (2002) obtained $\text{Fe II/Mg II} = 3.3\text{--}4.2$ for six quasars at $z \approx 3.4$ and $\text{Fe II/Mg II} = 3.8 \pm 0.4$ for a low- z composite quasar, while Thompson, Hill, & Elston (1999) measured $\text{Fe II/Mg II} \approx 6\text{--}7$ (over a slightly wider wavelength range of $2000\text{--}3000 \text{ \AA}$ for Fe II) for composite quasar spectra at $z = 3$ and $z = 4$, and 4.3 ± 0.1 for a low- z composite quasar. Our result is also within the same range as values measured by Iwamuro et al. (2002), Dietrich et al. (2003b), and Freudling et al. (2003) for quasars at $z = 4.4\text{--}6.3$.

Thus, the lack of any strong evolution in Fe II/Mg II noted by Thompson et al. out to $z = 3\text{--}4$ apparently continues out to $z = 6.4$; even at this redshift there is still no indication of a substantial decrease in this ratio. If the Fe II/Mg II flux ratio can be interpreted as even a rough indicator of the underlying abundance ratio, then the age of the universe at $z = 6.4$ provides some constraints on metal enrichment models. The minimum lifetime for SN Ia progenitors has often been considered to be $\sim 1\text{--}1.5 \text{ Gyr}$; this would imply that the Fe/ α abundance ratio should undergo a strong rise starting at $1\text{--}1.5 \text{ Gyr}$ following the first burst of star formation in which SN Ia progenitors are created (Hamann & Ferland 1993; Yoshii et al. 1998).

Observations of Fe II/Mg II ratios in quasars at $z \approx 4$ could still be consistent with such models (Dietrich et al. 2002), but our observations and those of Freudling et al. (2003) rule out

⁵ The Vestergaard & Wilkes (2001) iron template is not distributed or shared freely, so we re-created their template spectrum using information given in their published article.

models with iron enrichment timescales of $\gtrsim 800$ Myr. However, the timescale for the maximum SN Ia rate (and hence iron enrichment) depends sensitively on the star formation rate and initial mass function, and may be much shorter than the canonical 1 Gyr for an intense starburst in the core of a rapidly forming elliptical galaxy (Friaça & Terlevich 1998; Matteucci & Recchi 2001). The models of Friaça & Terlevich (1998) give a typical timescale of 0.3 Gyr to reach solar abundance of iron in the interstellar medium of a proto-elliptical galaxy; similarly, Matteucci & Recchi (2001) find that the peak SN Ia rate in an elliptical galaxy occurs ~ 0.3 Gyr after the major burst of star formation. If the iron abundance were built up in just 0.3 Gyr, then the SN Ia progenitors would have formed at $z \gtrsim 10$. There may be only a brief temporal window during which a quasar would exhibit a low Fe/ α abundance ratio, and this epoch could be at a redshift as high as ~ 10 if star formation began at $z \approx 20$ (e.g., Kogut et al. 2003). Alternatively, the iron may have been produced in pair-instability supernovae from Population III stars with initial masses of 140–260 M_{\odot} ; a single such explosion could produce up to 40 M_{\odot} of iron (Heger & Woosley 2002). This would result in iron enrichment of the pregalactic gas within a few Myr after the first burst of star formation.

3.2. The Mass of the Black Hole

The only practical methods to estimate the black hole masses in distant quasars are based on scaling relations derived from low-redshift samples. Reverberation mapping of Seyfert galaxies and quasars at $z < 0.4$ has demonstrated a correlation between continuum luminosity and BLR radius (Wandel, Peterson, & Malkan 1999; Kaspi et al. 2000). By combining the continuum luminosity with measurements of broad-line widths, the black hole mass can be estimated under the assumption of virial motion of the BLR clouds. The original scaling relations were derived from FWHM(H β) and the continuum luminosity at 5100 Å, but similar relations have been determined using ultraviolet continuum luminosity combined with the linewidth of either C IV (Vestergaard 2002) or Mg II (McLure & Jarvis 2002). These relations have the form $M_{\bullet} \propto [\lambda L_{\lambda}(\text{UV})]^{\beta} \times \text{FWHM}(\text{line})^2$, where $\beta = 0.47$ (McLure & Jarvis 2002) or 0.7 (Vestergaard 2002). The dominant uncertainty in the M_{\bullet} estimates comes from the intrinsic scatter in the M_{\bullet} -linewidth correlations, which is a factor of ~ 2.5 –3, rather than from measurement uncertainties on the linewidths.

Willott et al. (2003) found FWHM(Mg II) = 6000^{+1100}_{-600} km s $^{-1}$ based on a double-Gaussian fit with the two components fixed at rest wavelengths of 2796 and 2802 Å, giving $M_{\bullet} \approx 3 \times 10^9 M_{\odot}$. Our spectrum shows that the profile is rather asymmetric, and the full Mg II profile has FWHM(Mg II) = 5500 ± 200 km s $^{-1}$. Applying the McLure & Jarvis (2002) relation with $\lambda L_{\lambda}(3000 \text{ \AA}) = 5.7 \times 10^{39}$ W, we obtain $M_{\bullet} \approx 2 \times 10^9 M_{\odot}$. This result is close to the previous estimate by Willott et al., since we find similar values for FWHM(Mg II) and $L_{\lambda}(3000 \text{ \AA})$.

The peculiar shape of the C IV line might result from non-Keplerian kinematics, calling into question the application of the Vestergaard (2002) method to derive M_{\bullet} for this particular object. Keeping this caveat in mind, we will derive an M_{\bullet} estimate from the C IV line for purposes of comparison with the Mg II method. To measure FWHM(C IV), the spectrum was first prepared by subtracting off the Fe template, with its overall scaling determined by the fit to the K -band spectrum. The Fe emission only makes a small ($\sim 10\%$) contribution to the flux level in the continuum surrounding C IV. Then, the region from

1450 to 1630 Å rest wavelength was fit with a single Gaussian plus continuum. The best-fit Gaussian has FWHM(C IV) = 9000 ± 300 km s $^{-1}$. Vestergaard’s M_{\bullet} relation was derived assuming a cosmology with $H_0 = 75$ km s $^{-1}$ Mpc $^{-1}$, $q_0 = 0.5$, and $\Lambda = 0$. Taking $\lambda L_{\lambda}(1350 \text{ \AA}) = 2.5 \times 10^{46}$ erg s $^{-1}$ for these cosmological parameters, we obtain $M_{\bullet} \approx 6 \times 10^9 M_{\odot}$ for SDSS J1148+5251. Given that these scaling methods have an estimated uncertainty of a factor of 2.5–3, the two estimates of M_{\bullet} from Mg II and C IV are in reasonable agreement. It would still be worthwhile to obtain a C IV spectrum with higher S/N ratio to check the reality of the large blueshift and linewidth.

To estimate the bolometric luminosity, we apply a bolometric correction of $L_{\text{bol}}/[\nu L_{\nu}(2500 \text{ \AA})] = 6.3$, which is typical of low-redshift quasars (Elvis et al. 1994). This gives $L_{\text{bol}} \approx 4 \times 10^{47}$ erg s $^{-1}$ and implies (as previously shown by Willott et al.) an Eddington ratio of $L_{\text{bol}}/L_{\text{Edd}} \approx 1$ for $M_{\bullet} = 3 \times 10^9 M_{\odot}$.

A few additional caveats should be noted: the apparent luminosity of the quasar can be affected by dust extinction, continuum beaming, or gravitational lensing. Significant extinction is unlikely because the spectral shape of the quasar does not appear strongly reddened relative to the SDSS composite quasar, while Willott et al. (2003) argue against continuum beaming because the Mg II equivalent width is typical of unbeamed quasars. Lensing is expected to affect only a small fraction of high- z SDSS quasars (Wyithe & Loeb 2002; Pindor et al. 2003), and infrared images of SDSS J1148+5251 do not give any indication of lensing (Fan et al. 2003).

It is remarkable to find such a massive black hole at such a large look-back time. Nevertheless, models for the hierarchical growth of supermassive black holes by merging and gas accretion can accommodate masses of $> 10^9 M_{\odot}$ in quasars at $z \gtrsim 6$ if the seed black holes form at $z > 10$ (e.g., Haiman & Loeb 2001; Volonteri, Haardt, & Madau 2003). The initial seed black holes may be objects with $M_{\bullet} \approx 100$ –200 M_{\odot} formed by collapse of supermassive Population III stars (Fryer, Woosley, & Heger 2001; Madau & Rees 2001; Schneider et al. 2002). We note that even a single seed black hole having 180 M_{\odot} at $z = 20$ could (just barely) grow to $3 \times 10^9 M_{\odot}$ by $z = 6.4$ if it were constantly accreting at the Eddington luminosity with a radiative efficiency of $\epsilon = 0.1$, so the present data do not yet require multiple black hole mergers to build up the observed black hole mass.

4. CONCLUSIONS

The Keck spectra reveal an Fe II/Mg II ratio in SDSS J1148+5251 that is within the normal range for quasars at lower redshifts, indicating that substantial iron enrichment must have occurred in the densest regions of the universe at redshifts greater than 6.4. Recent photoionization calculations by Verner et al. (2003) have shown that Fe II/Mg II is not a straightforward diagnostic of Fe/ α abundance ratios, but useful constraints on the Fe/Mg abundance ratio can be derived from observations of the ultraviolet Fe II/Mg II ratio combined with the ratio of ultraviolet to optical Fe II strength. The rest-frame optical Fe II emission in very high-redshift quasars cannot be measured from the ground, but these measurements can be pursued in the future with the *James Webb Space Telescope*. Searches for quasars at still higher redshifts may provide a glimpse of the earliest epoch of iron production and give stringent constraints on the formation redshift of the seed black holes that were the progenitors of luminous quasars.

We thank D. Kelson for the use of his sky-subtraction code and D. Stern for helpful comments. Research by A.J.B. is supported by NASA through Hubble Fellowship grant #HST-HF-01134.01-A awarded by STScI. P.M. was supported by a Carnegie Starr Fellowship. Data presented herein were obtained at the W.M. Keck Observatory, which is operated as a

scientific partnership among Caltech, the University of California, and NASA. The Observatory was made possible by the generous financial support of the W.M. Keck Foundation. The authors wish to recognize and acknowledge the very significant cultural role and reverence that the summit of Mauna Kea has always had within the indigenous Hawaiian community.

REFERENCES

- Bertoldi, F., Carilli, C. L., Cox, P., Fan, X., Strauss, M. A., Beelen, A., Omont, A., & Zylka, R. 2003, *A&A*, in press
- Dietrich, M., Appenzeller, I., Vestergaard, M., & Wagner, S. J. 2002, *ApJ*, 564, 581
- Dietrich, M., Hamann, F., Shields, J. C., Constantin, A., Heidt, J., Jäger, K., Vestergaard, M., & Wagner, S. J. 2003a, *ApJ*, 589, 722
- Dietrich, M., Hamann, F., Appenzeller, I., & Vestergaard, M. 2003b, *ApJ*, in press
- Elvis, M., et al. 1994, *ApJS*, 95, 1
- Fan, X., et al. 2003, *AJ*, 125, 1649
- Freudling, W., Corbin, M. R., & Korista, K. T. 2003, *ApJ*, 587, L67
- Friřaça, A. C. S. & Terlevich, R. J. 1998, *MNRAS*, 298, 399
- Fryer, C. L., Woosley, S. E., & Heger, A. 2001, *ApJ*, 550, 372
- Haiman, Z., & Loeb, A. 2001, *ApJ*, 552, 459
- Hamann, F., & Ferland, G. 1993, *ApJ*, 418, 11
- Hamann, F., & Ferland, G. 1999, *ARA&A*, 37, 487
- Heger, A. & Woosley, S. E. 2002, *ApJ*, 567, 532
- Iwamuro, F., Motohara, K., Maihara, T., Kimura, M., Yoshii, Y., & Doi, M. 2002, *ApJ*, 565, 63
- Kaspi, S., Smith, P. S., Netzer, H., Maoz, D., Jannuzi, B. T., & Giveon, U. 2000, *ApJ*, 533, 631
- Kelson, D. D. 2003, *PASP*, 115, 688
- Kogut, A., et al. 2003, *ApJ*, in press
- Madau, P., & Rees, M. J. 2001, *ApJ*, 551, L27
- Marziani, P., Sulentic, J. W., Dultzin-Hacyan, D., Calvani, M., & Moles, M. 1996, *ApJS*, 104, 37
- Matteucci, F., & Recchi, S. 2001, *ApJ*, 558, 351
- McLean, I. S., Graham, J. R., Becklin, E. E., Figer, D. F., Larkin, J. E., Levenson, N. A., & Teplitz, H. I. 2000, *Proc. SPIE*, 4008, 1048
- McLure, R. J., & Jarvis, M. J. 2002, *MNRAS*, 337, 109
- Pindor, B., Turner, E. L., Lupton, R. H., & Brinkmann, J. 2003, *AJ*, 125, 2325
- Richards, G. T., Vanden Berk, D. E., Reichard, T. A., Hall, P. B., Schneider, D. P., SubbaRao, M., Thakar, A. R., & York, D. G. 2002, *AJ*, 124, 1
- Schneider, R., Ferrara, A., Natarajan, P., & Omukai, K. 2002, *ApJ*, 571, 30/
- Thompson, K. L., Hill, G. J., & Elston, R. 1999, *ApJ*, 515, 487
- Vacca, W. D., Cushing, M. C., & Rayner, J. T. 2003, *PASP*, 115, 389
- Vanden Berk, D. E., et al. 2001, *AJ*, 122, 549
- Verner, E., Bruhweiler, F., Verner, D., Johansson, S., & Gull, T. 2003, *ApJ*, 592, L59
- Vestergaard, M. 2002, *ApJ*, 571, 733
- Vestergaard, M., & Wilkes, B. J. 2001, *ApJS*, 134, 1
- Volonteri, M., Haardt, F., & Madau, P. 2003, *ApJ*, 582, 559
- Wandel, A., Peterson, B. M., & Malkan, M. A. 1999, *ApJ*, 526, 579
- White, R. L., Becker, R. H., Fan, X., & Strauss, M. A. 2003, *AJ*, 126, 1
- Willott, C. J., McLure, R. J., & Jarvis, M. J. 2003, *ApJ*, 587, L15
- Wyithe, J. S. B., & Loeb, A. 2002, *ApJ*, 581, 886
- Yoshii, Y., Tsujimoto, T., & Kawara, K. 1998, *ApJ*, 507, L113

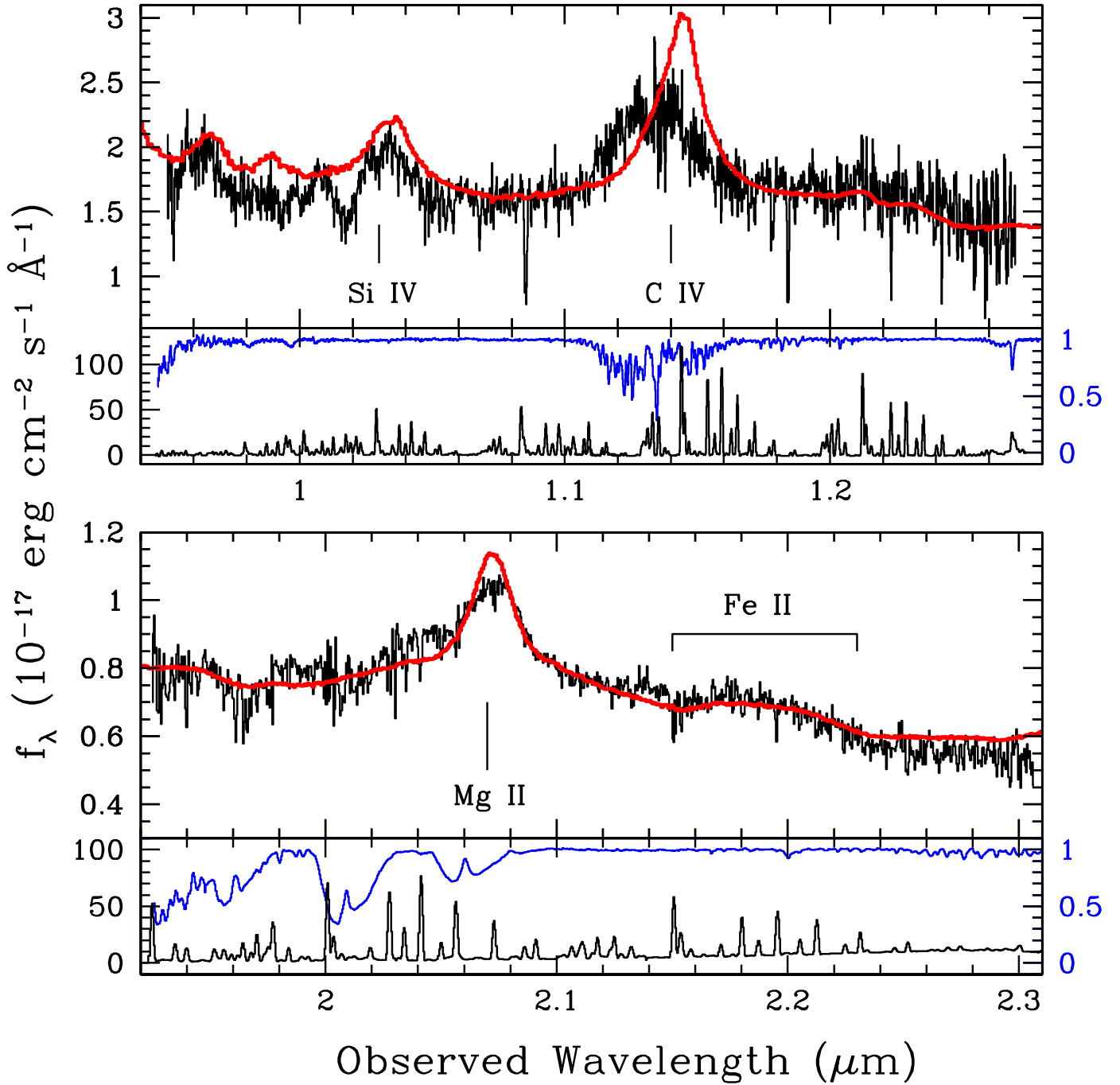


FIG. 1.— Near-infrared spectra of SDSS J1148+5251. The upper panels show the combined NIRSPEC-1 and 2 settings, and the lower panels show the NIRSPEC-6 setting. The spectrum overplotted on that of SDSS J1148+5251 is the SDSS composite quasar of Vanden Berk et al. (2001), transformed to $z = 6.40$. The same scaling factor has been applied to the SDSS composite quasar in both spectral regions. The panels below the quasar spectra show the atmospheric transmission and the night sky emission spectra. The Si IV, C IV, and Mg II emission lines are labelled. There is iron emission throughout this spectral region; the prominent iron blend at 2900–3000 Å rest wavelength is labelled.

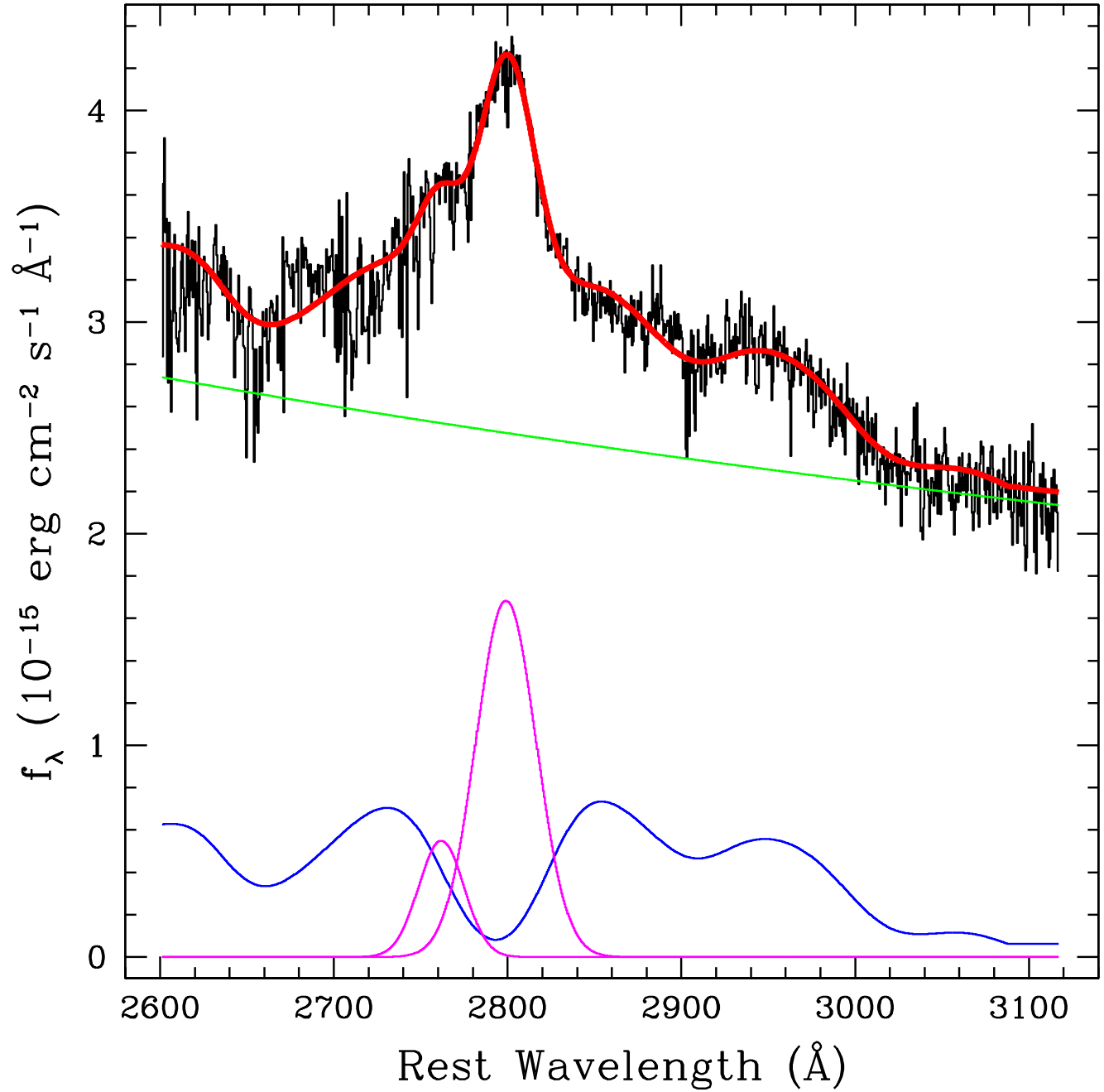


FIG. 2.— Model fit to the Mg II spectral region. The double-Gaussian model for the Mg II profile, the broadened Fe emission template, and the power-law continuum are displayed individually, and the full model is overlotted on the quasar spectrum. The observed spectrum has been shifted to the rest frame and the flux density has been scaled by $(1+z)^3$.